Available online at www.sciencedirect.com
ScienceDirect
ELSEVIER
JOURNAL OF RARE EARTHS, Vol. 34, No. 9, Sep. 2016, P. 895
JOURNAL OF RARE EARTHS
www.re-journal.com/en/

Role of Nd_2O_3 nanoparticles addition on microstructural and superconducting properties of $YBa_2Cu_3O_{7-\delta}$ ceramics

Aima Ramli[1,2], Abdul Halim Shaari[1,*], Hussein Baqiah[1], Chen Soo Kean[1], Mohd Mustafa Awang Kechik[1], Zainal Abidin Talib[1]

(1. Superconductivity and Thin Films Laboratory, Department of Physics, Universiti Putra Malaysia, 43400 Serdang, Selangor, Malaysia; 2. Department of Physics, School of Fundamental Science, Universiti Malaysia Terengganu (UMT), 21030 Kuala Terengganu, Terengganu, Malaysia)

Received 27 January 2016; revised 17 May 2016

Abstract: The effects of Nd_2O_3 nanoparticles addition on microstructure, transport and AC susceptibility properties of $YBa_2Cu_3O_{7-\delta}$ (Y123) superconductors were systematically investigated using X-ray diffraction (XRD), scanning electron micrograph (SEM), four point probe measurement and AC spectrometer. It was found that the added samples were predominant by Y-123 phase beside small amount of Y-211 and unreacted Nd_2O_3 secondary phases. All added samples preserved the orthorhombic structure similar to the pure sample and no orthorhombic-to-tetragonal transition occurred. The samples became more porous and their grain size significantly decreased with addition of Nd_2O_3. The addition of nano-Nd_2O_3 disturbed the grain growth of Y123, thus resulting in the degradation of superconducting properties of the samples. The superconducting transition temperature ($T_{c\ onset}$) of samples decreased from 92 K for x=0.0 to 78 K for x=1.0 wt.%, which could be attributable to oxygen vacancy disorder. From AC susceptibility result, the inter- and intra-granular loss peaks became wider and broader with increase of Nd_2O_3 addition due to the weakening of grains coupling. On the other hand, the inter-granular critical current density, J_{cm}, was found to increase with Nd_2O_3 addition and had the highest value at x=0.6, confirming that Nd_2O_3 nanoparticles acted as pinning centers in Y123 matrix.

Keywords: YBCO; critical temperature; co-precipitation; AC susceptibility; critical current density; rare earths

$YBa_2Cu_3O_{7-\delta}$ (Y123) is one of the most important copper oxide based superconductors that has received great attention since it was discovered by Wu et al. in 1987[1]. Basically, this material is type II superconductors, which are characterized by three parameters: critical temperature, T_c, critical magnetic field, H_{c2}, and critical current J_c, for which the enhancement of these parameters is the key of technology application. The $YBa_2Cu_3O_{7-\delta}$ (Y123) system is one of the promising materials because its superconducting properties can be invested towards superconductor's technology application[2]. However, the bulk Y123 suffers from low grain boundary conductivity and poor flux pinning resulting in low J_c in the presence of magnetic field[3]. The main objective of research in Y123 is to increase J_c in the presence of magnetic field to achieve high value required by technological applications[4,5].

The incorporation of nano-size secondary phase into Y123 system improves its current carrying capability[6]. This is because of nano-size secondary phases acting as pinning centres that prevent the motion of magnetic flux, *i.e.* flux pining, and hence prevent suppression of J_c[2]. For this purpose, several nano-sized secondary phases have been introduced to bulk[7] and thin film Y123[8,9]. On the other hand, the addition of nano-size particles is expected to change other superconducting properties of Y123, *i.e.* T_c, due to locally modifying the crystalline structure and generate defects such as twins, tweed, and inhomogeneous micro-defects[7]. It has been reported that the addition of Al_2O_3 resulted in the decrease of T_c of Y123 while enhanced the J_c[7]. Furthermore, the addition of Hf_2O_3 nanoparticles was found to introduce $YBa_2HfO_{5.5}$ phase that acts as pinning centre for Y123 resulting in the enhancement of J_c[4]. Y123 can be classified as one member of family of $RBa_2Cu_3O_7$ superconductors in which R=Y and rare earth elements. Rare earth oxide particles such as Yb_2O_3, Ho_2O_3 and Gd_2O_3 were found to act as effective pinning centres in YBCO matrix[10–12]. It is interesting to explore the effect of Nd_2O_3 rare earth oxide nanoparticles addition on structural and superconducting properties of Y123 ceramics because Nd ions has high solubility in Y123 matrix[13–15]. Hence in this work, we reported the results of superconducting properties of $YBa_2Cu_3O_{7-\delta}$ with inclusion of small range Nd_2O_3, x=0.0–1.0 wt.%. The samples were prepared by using co-precipitation method. The results on crystal structure and phase formation analysis, morphology, transport and AC susceptibility were reported as well.

Foundation item: Project supported by Exploratory Research Grants Scheme (ERGS) (5527047), University Putra Malaysia through the Putra Grant (9440100), Ministry of Education Malaysia (MOE) and University Malaysia Terengganu (UMT)

* **Corresponding author:** Abdul Halim Shaari (**E-mail:** ahalim@upm.edu.my; **Tel.:** +603-89466648)

DOI: 10.1016/S1002-0721(16)60112-6

1 Experimental

1.1 Materials and samples preparation

Powder of constituent metal acetates of yttrium(III) acetate ($Y(CH_3COO)_3{\cdot}4H_2O$), barium acetate ($Ba(CH_3COO)$) and copper(II) acetate ($Cu(CH_3COO)_2$) with purity>99%, were weighed in their molar ratio of 1:2:3 and dissolved in acetic acid, namely solution A. Meanwhile, solution B containing 0.5 mol/L oxalic acid was prepared in a mixture of deionized high-purity water: isopropanol (*v*/*v*=1:1.5). Solution B was added drop-wise into solution A in an ice bath with continuous stirring in order to completely dissolve the solutions. A uniform, stable, blue suspension was formed and the slurry was filtered after 5–10 min of reaction. After filtration, the filtrated cake was allowed to dry at 80 ºC overnight. The dried blue precipitates were ground prior to thermal treatment at 900 ºC in air for 15 h. The calcined powders were added with nano-Nd_2O_3 (x=0.0–1.0 wt.%) and reground in an agate mortar until well-mixed. The mixed powders were pressed into pellets of 13 mm diameter using Specac manually operated hydraulic press. The pellets were sintered at 920 ºC for 15 h in air and cooled slowly to room temperature in a furnace at a rate 1 ºC/min.

1.2 Characterization and measurements

The structure and phase identification of the powder samples ground from sintered pellets were examined by powder XRD using a Philips 1710 diffractometer with Cu Kα radiation. Refinement of the X-ray diffraction data was carried out by the Rietveld method. The electrical resistance measurements were made by using standard four-probe method, in a closed cycle helium cryostat at temperatures between 20 and 300 K. The surface morphology of the samples was carried out by scanning electron micrograph (SEM). The AC susceptibility measurement was performed using a Cryogenic Balanced Inductive Detector (CryoBIND) SR830 lock-in-amplifier at a frequency of 123 Hz to study the flux penetration when the samples were heated from 75 to 95 K with the applied field ranging from 0.005 to 3.0 Oe.

2 Results and discussion

X-ray diffraction patterns of $YBa_2Cu_3O_{7-\delta}$ with addition of Nd_2O_3 are shown in Fig. 1. It is shown that the pure sample has single-phase of $YBa_2Cu_3O_{7-\delta}$ (Y123) with orthorhombic *Pmmm* structure. However, secondary phases belonged to Y211 and unreacted Nd_2O_3 emerged with addition of the Nd_2O_3 (x=0.2 wt.%–1.0 wt.%). This Y211 secondary phase is a semiconducting phase that belongs to Y_2BaCuO_5, which is commonly observed to coexist with Y123 phase. The lattice parameters *a*, *b*, and *c* and unit cell volume samples are listed in Table 1. The unit cell volume, *V*, varies as *x* increases. Table 1 depicts

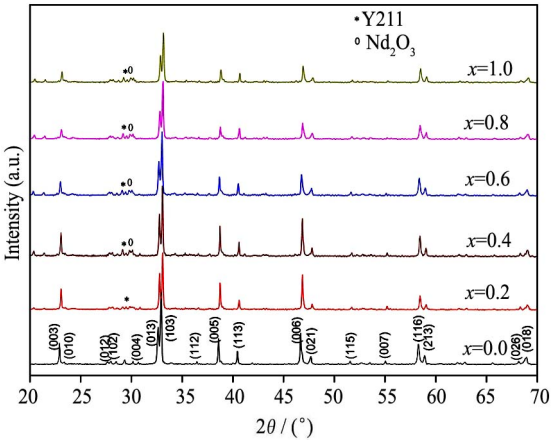

Fig. 1 X-ray diffraction patterns of $YBa_2Cu_3O_{7-\delta}$ samples with various additions of Nd_2O_3

Table 1 Lattice parameters of *a*, *b* and *c* axes amd unit cell volume of YBCO with Nd_2O_3 content, *x*

Nd_2O_3 (x)/wt.%	*a*/nm	*b*/nm	*c*/nm	*V*/nm	Orthorhombicity [(*a*–*b*)/(*a*+*b*)]
0.0	0.38211	0.38881	1.1690	0.1736762	0.00869
0.2	0.38210	0.38860	1.1687	0.1735333	0.00843
0.4	0.38220	0.38891	1.1686	0.1737015	0.00870
0.6	0.38231	0.38896	1.1692	0.1738650	0.00862
0.8	0.38249	0.38899	1.1695	0.1740097	0.00843
1.0	0.38245	0.38911	1.1694	0.1740304	0.00863

the change of lattice parameters as a function of Nd_2O_3 addition percentage. The lattice constant *a* increases while lattice constant *b* slightly decreases in sample x= 0.2 wt.% but increases in sample with x=0.4 wt.%–1.0 wt%. The orthorhombicity of samples, defined as [(*a*–*b*)/(*a*+*b*)], is depicted in Table 1[16]. The changes of lattice constants *a* and *b* diminish the orthorhombicity. However, all the added samples are conserved with the orthorhombic structure similar to the pure sample and no orthorhombic-to-tetragonal transition occurs. The variation in lattice parameters (*a*, *b*, *c*) and unit cell volume with increasing Nd_2O_3 concentration show that Nd^{3+} may be incorporated into the crystal structure of Y123. It was reported that the Nd^{3+} (0.0995 nm) ions are highly preferred to occupy the Ba-sites in Y123 system[13]. On the other hand, the addition of Nd_2O_3 may result in change of the oxygen content (δ) in Y123 system, which is another factor that affects the lattice constant[17,18].

Fig. 2 shows the normalized resistance versus temperature plots. The pure sample shows metallic behaviour in the normal state above the $T_{c\text{-onset}}$. The addition of Nd_2O_3 in the range of x=0.2–0.8 affects the metallic behavior of the normal state of samples that finally exhibited semiconducting like behavior for sample with x=1. Furthermore, the samples with $x\leq0.4$ show a single step transition, indicating that the samples are highly composed of Y123 phase. On the other hand, samples with x=0.6 wt.%–1.0 wt.% show a double step transition, at-

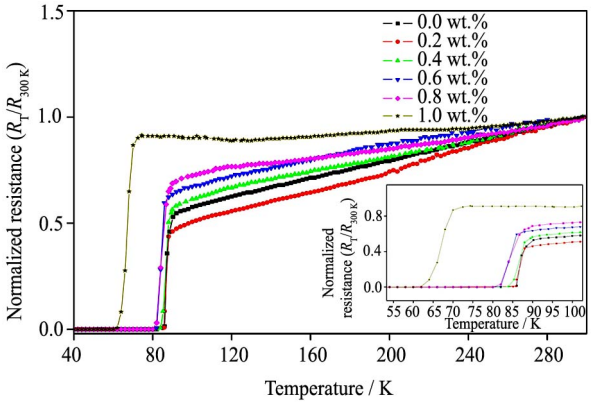

Fig. 2 Normalized electrical resistance versus temperature curve of $YBa_2Cu_3O_{7-\delta}$ samples with x=0.0–1.0 Nd_2O_3 additions

tributed to the presence of Y211 and Nd_2O_3 phases as confirmed by XRD data. The critical temperature, $T_{c\text{-onset}}$ for samples with x=0.0, 0.2, 0.4, 0.6, 0.8 and 1.0 are 92, 90, 89, 88, 87 and 74 K, respectively. The depression of T_c with Nd_2O_3 addition may be due to degradation of superconductors matrix by Nd_2O_3 addition as inferred from microstructure result below[10,11]. This could cause a reduction in oxygen content in the CuO chains that control the T_c in Y123 system due to cation substitution or movements of apical oxygen O(1). The apical oxygen between the CuO_2 plane and the Cu–O chain is known to play an important role in the hole distribution between the two layers[7]. The superconducting regions in high temperature superconductor show a maximum value of T_c at the optimal doping level, and a lower value in the overdoped region. It is well known that a parabolic relationship holds between the superconducting transition temperature, T_c and the hole concentrations, p[19]. The T_c appears to be maximized with hole concentration, p= 0.16. The carrier (number of holes) concentration-critical temperature dependence can be described by using the relation[20]:

$$T_{c\text{-onset}}/T_{c\text{-max}}=1-82.6(p-0.16)^2 \quad (1)$$

The hole concentrations of the samples were calculated and the results are shown in Table 2.

Fig. 3 shows the SEM images of YBCO with addition of Nd_2O_3, x=0.0–1.0 wt.%. The average sizes of grain for the samples were determined from 100 grains with magnification 1000X measured randomly using Image *J* software. As illustrated, there are changes in the grain size as well as the number of pores. The pure sample has the highest bulk density and the grains in the sample are strongly linked with no pores. The sample becomes porous and the grain size decreases from 1.825 to 1.292 μm when added with Nd_2O_3, x=0.2 wt.%–1.0 wt.%. The addition of Nd_2O_3 prevents the growth of YBCO grains, thus resulting in degradation of superconducting properties of the samples.

Since superconductor polycrystalline samples are granular in nature, the best way to study their superconducting properties is by using magnetization measurements rather than transport measurements. Ac susceptibility is considered as a non-destructive method, without

Table 2 Superconducting properties and hole concentrations for samples $YBa_2Cu_3O_{7-\delta}$ with various additions of x, Nd_2O_3

Nd_2O_3, x/wt.%	$T_{c\text{-onset}}$/K	$T_{c\text{-offset}}$/K	ΔT_c/K	Hole concentrations, p
0.0	92	88	4	0.160
0.2	90	86	4	0.144
0.4	89	83	6	0.140
0.6	88	82	6	0.137
0.8	87	80	7	0.130
1.0	74	62	12	0.110

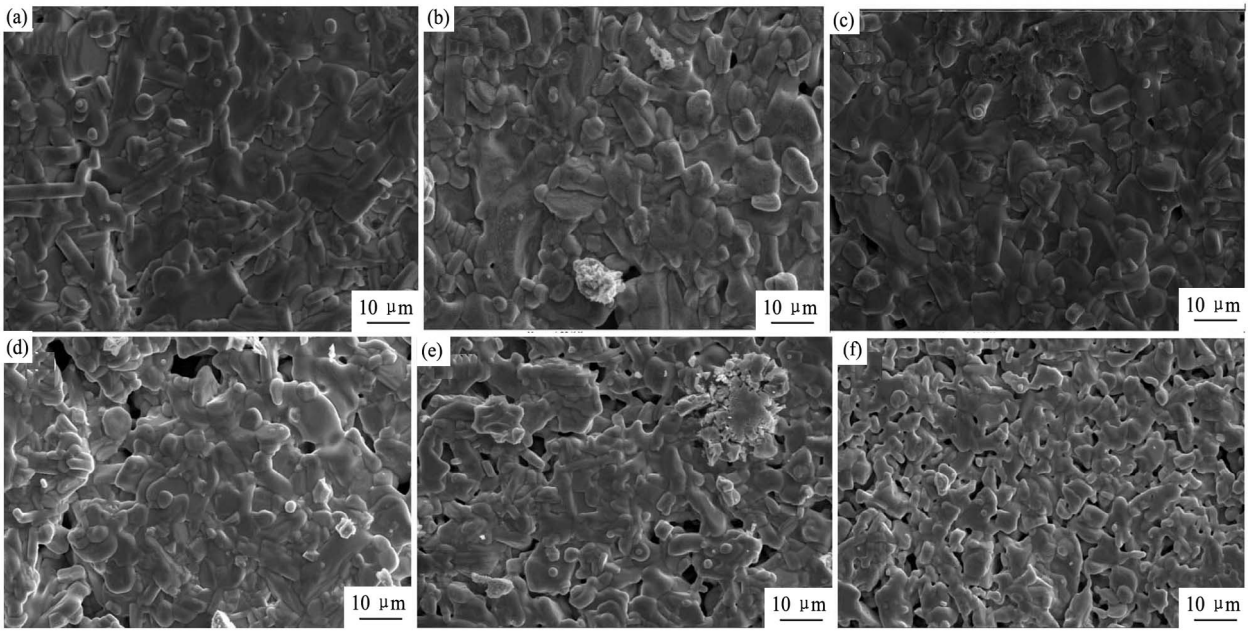

Fig. 3 SEM images with average grain size measured from image *J* for polished surface YBCO with various additions of Nd_2O_3 (a) 0; (b) 0.2; (c) 0.4; (d) 0.6; (e) 0.8; (f) 1.0

electrical contacts and the sample size can be very small yet in the powder form[21]. In polycrystalline HTS, a typical characteristic of AC susceptibility of superconductors is the appearance of a two-step diamagnetic transition in real susceptibility, i.e. χ', and double peaks of imaginary susceptibility, i.e. χ", due to the intra-granular and inter-granular transition. Fig. 4 shows the AC susceptibility of Y123 added with Nd_2O_3 (x= 0.0–1.0 wt.%) at the frequency of 123 Hz with various applied fields, H_{ac}; 0.005, 0.01, 0.05, 0.1, 0.5, 1.0, 2.0 and 3.0 Oe. The experimental AC susceptibility data χ' (T) and χ"(T) were normalised to $|\chi|$ at the lowest temperature and the lowest AC field amplitude for each sample since the demagnetising correction would cause χ'=–1. Double-step transitions in χ'(T) were observed, related to the flux removal from the inter-grain and intra-grain regions of the YBCO superconductor[22]. This is a characteristic behaviour of cuprate superconductors due to its granular nature. The imaginary part χ"(T) shows the inter-granular loss peaks that are sharper and narrower at low field as compared to high field. The loss peaks tend to shifting to lower temperature and broadens when the H_{ac} increased. The larger peak shift means the weaker flux pinning ability of the system[23].

Table 3 shows the summarized data of onset temperature of diamagnetism, $T_{c\text{-}on}$, coupling peak temperature, T_p, phase lock-in temperature (onset of decoupling of the grains associated with the lower transition temperature in (χ'–T), T_{cj}, and Josephson current, I_o, at 123 Hz with various amounts of Nd_2O_3. The $T_{c\text{-}on}$ is about 91 K, which is constant at different field amplitudes for each samples. The AC field at this temperature is high enough to penetrate inside the grains. At extremely low temperature, the innermost of the samples is expected to be shielded by the supercurrent and hence, χ'(T) curves saturate. The saturation of diamagnetic transition shifts towards low temperature with increasing field[5].

In imaginary part, χ"(T), there are two major peaks as

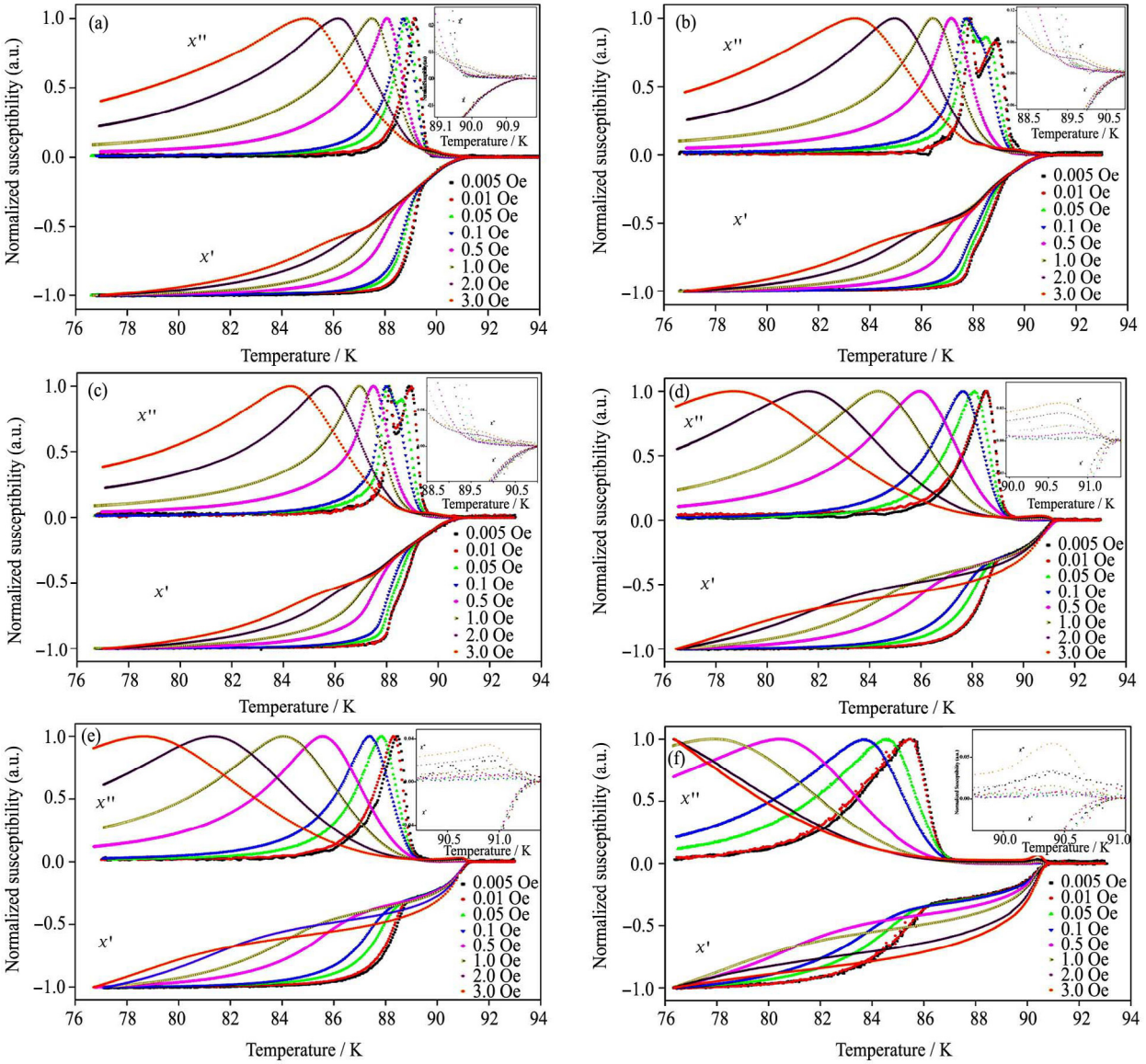

Fig. 4 AC susceptibility of YBCO added with Nd_2O_3 (0.0 wt.% (a), 0.2 wt.% (b), 0.4 wt.% (c), 0.6 wt.% (d), 0.8 wt.% (e) and 1.0 wt.% (f)) at the frequency of 123 Hz and various applied fields

Table 3 Summarized data of coupling peak temperature, T_p, onset temperature of diamagnetism, $T_{c\text{-}on}$, phase lock-in temperature, T_{cj} and Josephson current, I_o at 123 Hz with various amounts of Nd_2O_3

Sample (x)/	T_p/K									$T_{c\text{-}on}$/K	T_{cj}/K	I/μA
wt.%	H_{ac}/Oe	0.005	0.01	0.05	0.1	0.5	1	2	3			
0.0		89.2	89.2	88.9	88.7	88.1	87.5	86.2	85.0	91.1	88.1	47.65
0.2		87.9	87.9	87.8	87.8	87.2	86.5	85.0	83.4	90.7	87.6	54.67
0.4		88.9	89.0	88.1	87.9	87.5	86.9	85.7	84.3	90.6	87.6	47.26
0.6		88.6	88.6	88.1	87.7	85.9	84.3	81.6	78.7	90.5	87.4	45.83
0.8		88.4	88.3	87.9	87.4	85.6	84.1	81.4	78.8	90.2	87.0	43.99
1.0		85.3	84.5	84.6	83.8	80.4	77.8	–	–	90	86.8	43.48

can be seen in samples x=0.2 wt.%–0.4 wt.% at 0.005 and 0.01 Oe. However, both peaks merge together and form one broad peak at samples x=0.6 wt.%–1.0 wt.%. The dissipative intra-granular peak is weakly affected by the change of the ac amplitude for the whole sample thus it is difficult to be determined due to the overlapping with the inter-granular transition. As can be seen, the intra-granular peak is more pronounced at higher Nd_2O_3 additives (x≥0.6 wt.%) and the highest field (H_{ac}≥2 Oe), but the inter-granular losses peak is not visible as it is below minimum temperature measurement range. Wide and broad separation of inter- and intra-granular loss peaks shows that the grains are not well-coupled as the additives increased. Peak temperature, T_p, at imaginary part of susceptibility curve is the temperature where the maximum energy loss occurred when the vortices fully penetrated the sample. $T_{p\text{-inter}}$ and $T_{p\text{-intra}}$ ($T_{p\text{-inter}}$< $T_{p\text{-intra}}$) represent maximum hysteresis loss due to the motion of inter-granular Josephson and intra-granular (Abrikosov) vortices, respectively[21]. Due to weakened pinning force density and lower screening currents, the T_p shifted to lower temperature as the applied field amplitude and adding concentration of Nd_2O_3 increased[23].

It is known that maximum losses occur when the flux lines penetrate as the applied field reaches at the centre of the samples, at peak temperature (T_p) of χ" the applied field is considered as full penetration field. Hence, according to the Bean model[24], the critical current density J_c, as a function of the peak temperature (T_p), can be defined as: J_c (T_p)=H_{ac}/a~$H_{ac}/\sqrt{ab}$, where for rectangular bar shaped cross section of sample is $2a$×$2b$ and H_{ac} is the amplitude of applied AC field. The resulting magnetic field-dependent inter-granular critical current densities, J_{cm}, for samples with different Nd_2O_3 contents, x= 0.0–1.0 wt.% are depicted in Fig. 5. The J_{cm} of samples enhanced with increasing Nd_2O_3 addition in the range x= 0.0−0.6. Samples with x=0.6 wt.% shows the highest J_{cm} value at different applied magnetic fields. The highest value of J_{cm}, 5.77×10^5 A/cm^2, has been achieved at the lowest magnetic field, *i.e.* 0.005 Oe, for sample with x=0.6. While at the highest magnetic field, *i.e.* 3 Oe, the J_{cm} of sample with x=0.6 equals to 1.91×10^3 A/cm^2 which is three times higher than that of pure samples.

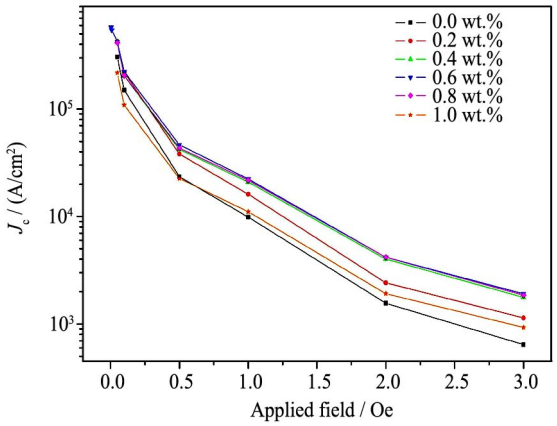

Fig. 5 Values of J_{cm} versus H_{ac} for the YBCO added with Nd_2O_3 at x=0.0–1.0 wt.%

This enhancement of J_{cm} could be related to the introduction of pinning centre in YBCO system by Nd_2O_3 addition. On the other hand, the J_{cm} decreased by further increase of the content of Nd_2O_3 above x=0.6, which could be attributed to the weakening of the inter-granular coupling due to pore-like structures observed in SEM micrograph.

3 Conclusions

The $YBa_2Cu_3O_{7-\delta}$ ceramics added with nano-Nd_2O_3 (0≤x≤1.0 wt.%) were successfully synthesized via co-precipitation method. From the refinement of XRD data using Rietveld refinement, it was found that the samples were predominantly single phase perovskite structure Y-123 with orthorhombic and secondary phase, Y-211 for x≥0.2 wt.%. The scanning electron microscopy (SEM) result showed that the pure sample had the highest bulk density and the grains in the sample were strongly linked with no pores. For samples with x=0.2 wt.%–1.0 wt.%, structure became more porous and the grain sizes significantly decreased. The addition of nano-Nd_2O_3 might induce oxygen vacancy disorder that resulted in reduction of the T_c from 92 K for x=0.0 to 78 K for x=1.0. From AC susceptibility measurement, the intergranular peaks became broadened and widened as the applied field increased from 0.005 to 3.0 Oe with additions of Nd_2O_3 (0.0 wt.% to 1.0 wt.%) as a result of weakening of

grains coupling. On the other hand, the inter-granular critical current density, J_{cm}, increased with optimum value, 5.77×10^5 A/cm^2 at 0.005 Oe magnetic applied filed for sample with x=0.6 confirming that Nd_2O_3 nanoparticles acted as pinning center in Y123 matrix.

Acknowledgments: The authors would like to thank the valuable supports and discussions by all members of Superconductor and Thin Film Laboratory of University Putra Malaysia.

References:

[1] Wu M-K, Ashburn J R, Torng C J, Hor P H, Meng R L, Gao L, Huang Z J, Wang Y, Chu C. Superconductivity at 93 K in a new mixed-phase Y-Ba-Cu-O compound system at ambient pressure. *Phys. Rev. Lett*., 1987, **58**: 908.

[2] Haugan T, Barnes P N, Wheeler R, Meisenkothen F, Sumption M. Addition of nanoparticle dispersions to enhance flux pinning of the $YBa_2Cu_3O_{7-x}$ superconductor. *Nature*, 2004, **430**: 867.

[3] Maple M B. High-temperature superconductivity. *J. Magn. Magn. Mater.*, 1998, **177-181**, Part 1: 18.

[4] Rejith P P, Vidya S, Vipinlal, Solomon S, Thomas J K. Flux-pinning properties of nanocrystalline HfO_2 added $YBa_2Cu_3O_{7-\delta}$ superconductor. *Phys. Status Solidi B*, 2014, **251**: 809.

[5] Öztürk A, Düzgün İ, Çelebi S. The effect of partial Lu doping on magnetic behaviour of YBCO (123) superconductors. *J. Alloys Compd*., 2010, **495**: 104.

[6] Strickland N M, Long N J, Talantsev E F, Hoefakker P, Xia J, Rupich M W, Kodenkandath T, Zhang W, Li X, Huang Y. Enhanced flux pinning by $BaZrO_3$ nanoparticles in metal-organic deposited YBCO second-generation HTS wire. *Physica C*, 2008, **468**: 183.

[7] Mellekh A, Zouaoui M, Ben Azzouz F, Annabi M, Ben Salem M. Nano-Al_2O_3 particle addition effects on $YBa_2Cu_3O_y$ superconducting properties. *Solid State Commun*., 2006, **140**: 318.

[8] Polat Ö, Ertuğrul M, Thompson J R, Leonard K J, Sinclair J W, Paranthaman M P, Wee S H, Zuev Y L, Xiong X, Selvamanickam V, Christen D K, Aytu T. Superconducting properties of $YBa_2Cu_3O_7$ films deposited on commercial tape substrates, decorated with Pd or Ta nano-islands. *Supercond. Sci. Technol*., 2012, **25**: 025018.

[9] Varanasi C V, Barnes P N, Burke J. Enhanced flux pinning force and uniquely shaped flux pinning force plots observed in $YBa_2Cu_3O_{7-x}$ films with $BaSnO_3$ nanoparticles. *Supercond. Sci. Technol*., 2007, **20**: 1071.

[10] Xu S, Yu A P, Gu Y N, Wu X S. Effect of Yb_2O_3 additives on structure and transport properties of $YBa_2Cu_3O_{7-\delta}$. *J. Rare Earths*, 2010, 28(Suppl. 1): 434.

[11] Xu S, Wu X S, Ma G B, Wang Z H, Gao J. Effects of Gd_2O_3 addition in $YBa_2Cu_3O_{7-\delta}$ on the critical current density. *J. Appl. Phys*., 2008, **103**: 07C714.

[12] Xu S, Gu Y N. Effect of Ho_2O_3 additives on $YBa_2Cu_3O_{7-\delta}$ properties. *Adv. Sci. Lett.*, 2012, **5**: 310.

[13] Tang W H, Gao J. Influence of Nd at Ba-sites on superconductivity of $YBa_{2-x}Nd_xCu_3O_y$. *Physica C*, 1998, **298**: 66.

[14] Ramteke D D, Annapurna K, Deshpande V K, Gedam R S. Effect of Nd^{3+} on spectroscopic properties of lithium borate glasses. *J. Rare Earths*, 2014, **32**: 1148.

[15] Li X W, Li M, Wang M T, Liu Z G, Hu Y H, Tian J H. Effects of neodymium and gadolinium on weathering resistance of ZnO-B_2O_3-SiO_2 glass. *J. Rare Earths*, 2014, **32**: 874.

[16] Giri R, Awana V P S, Singh H K, Tiwari R S, Srivastava O N, Gupta A, Kumaraswamy B V, Kishan H. Effect of Ca doping for Y on structural/microstructural and superconducting properties of $YBa_2Cu_3O_{7-\delta}$. *Physica C*, 2005, **419**: 101.

[17] Wu X S, Xiang X H, Chen W M, Li Y, Liu W J, Jiang S S. Structural anomalies in $LaBa_2Cu_3O_x$ cuprates with iron substitution. *Physica C*, 1998, **301**: 29.

[18] Benzi P, Bottizzo E, Rizzi N. Oxygen determination from cell dimensions in YBCO superconductors. *J. Cryst. Growth*, 2004, **269**: 625.

[19] Terzioglu C, Aydin H, Ozturk O, Bekiroglu E, Belenli I. The influence of Gd addition on microstructure and transport properties of Bi-2223. *Physica B*, 2008, **403**: 3354.

[20] Tallon J L, Bernhard C, Shaked H, Hitterman R L, Jorgensen J D. Generic superconducting phase behavior in high-T_c cuprates: T_c variation with hole concentration in $YBa_2Cu_3O_{7-\delta}$. *Phys. Rev. B*, 1995, **51**: 12911.

[21] Sharma D, Kumar R, Awana V P S. DC and AC susceptibility study of sol-gel synthesized $Bi_2Sr_2CaCu_2O_{8+\delta}$ superconductor. *Ceram. Int.*, 2013, **39**: 1143.

[22] Rani P, Jha R, Awana V P S. AC Susceptibility study of superconducting $YBa_2Cu_3O_7$:Ag_x bulk composites (x= 0.0–0.20): The role of intra and intergranular coupling. *J. Supercond. Novel Magn.*, 2013, **26**: 2347.

[23] Çelebi S, Kölemen U, Malik A I, Öztürk A. Effect of ZnO additions on the magnetic behaviour in YBCO superconductors. *Phys. Status Solidi A*, 2002, **194**: 260.

[24] Bean C. Magnetization of high-field superconductors. *Rev. Mod. Phys.*, 1964, **36**: 31.